Supplementary information for

Single-Shot Spatial-Temporal-Spectral Complex Amplitude Imaging via Wavelength-Time Multiplexing

YINGMING XU,[1,4,6] CHENGZHI JIN,[2,5,6] LIANGZE PAN,[3] YU HE,[2] YUNHUA YAO,[2] DALONG QI,[2,7] CHENG LIU,[4,8] JUNHUI SHI,[1,*] ZHENRONG SUN,[2] SHIAN ZHANG,[2] AND JIANQIANG ZHU[4]

[1]*Research Center for Novel Computational Sensing and Intelligent Processing, Zhejiang Lab, Hangzhou 311100, China.*
[2]*State Key Laboratory of Precision Spectroscopy, School of Physics and Electronic Science, East China Normal University, Shanghai 200241, China.*
[3]*College of Optical and Electronic Technology, China Jiliang University, Hangzhou, Zhejiang 310018, China.*
[4]*Key Laboratory of High Power Laser and Physics, Shanghai Institute of Optics and Fine Mechanics, Chinese Academy of Sciences, Shanghai 201800, China.*
[5]*College of Electronics and Information Engineering, South-Central Minzu University, Wuhan 430074, China*
[6]*These authors contributed equally to this work.*
[7]*dlqi@lps.ecnu.edu.cn*
[8]*chengliu@siom.ac.cn*
junhuishi@outlook.com

Supplementary Note I Phase information of the encoding plate at different wavelengths

The encoding plate forms phase modulation on the light field through a phase step of random distribution. Therefore, its phase modulation amount depends on the delay of step. According to formula $\phi_\lambda = \dfrac{790}{\lambda}\phi_{790}$, for an encoding plate, the phase modulation amount for different wavelengths varies differently. Therefore, the phase modulation of encoding plate of different wavelengths needs to be corrected. The FWHM of the spectral resolution corresponding to the reconstructed 50-frame images shown in the Visualization 1 is 0.8 nm. At the same time, the complex amplitude distributions of the encoding plates at three wavelengths are shown in Fig. S1. Figs. S1(a) to S1(c) are the complex amplitude distributions corresponding to wavelengths of 769 nm, 790 nm, and 808 nm, and the phase modulation differences at points P and Q are 2.56 rad, 2.5 rad and 2.44 rad, respectively.
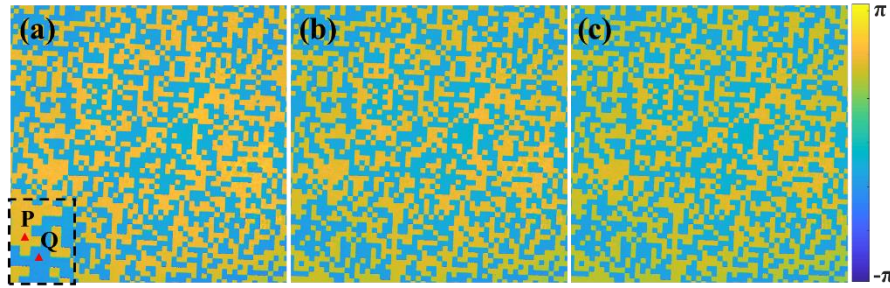

Fig. S1 Phase modulation distribution diagrams of the encoding plate corresponding to wavelengths of 769 nm (a), 790 nm (b) and 808 nm (c).

Supplementary Note II Variation in the rotation angle of the spatial vortex pulse phase

The phase distribution of the ultrashort spatial vortex pulse rotates with time, as shown by the rotating vector $\vec{\theta}$ in Fig. S2. It rotates along the $\vec{\theta}_{t3}$ direction in the time range of -100 ps - 20 ps, but rotates along the $\vec{\theta}_{t9}$ direction in the range of 40 ps - 80 ps. For different wavelengths, the rotation angle of the corresponding phase topological charge is smaller than the intensity distribution. The corresponding angle variation range is expressed as: $\vec{\theta}$ =[35 °, 28 °, 22 °, 20 °, 19 °, 16 °, 14 °, 7 °, 10 °, 13 °]. The one-dimensional curve depicting the variation in angle is illustrated in Fig. S3, with the inflection point of the angle rotation occurring at 40 ps.
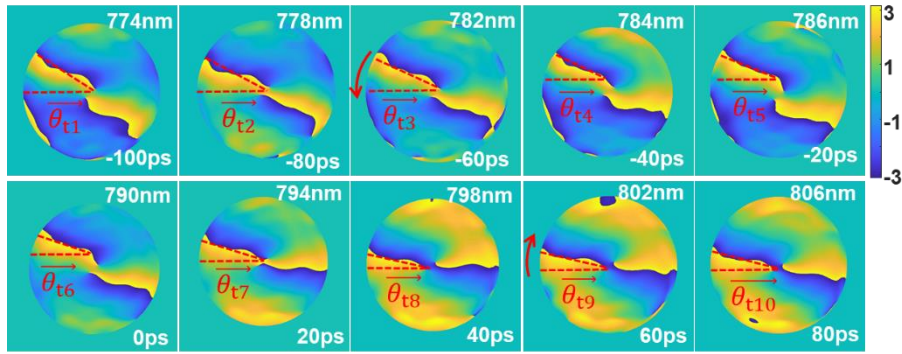
Fig. S2 Phase distribution of the spatial vortex pulse reconstructed by STS-CAI.
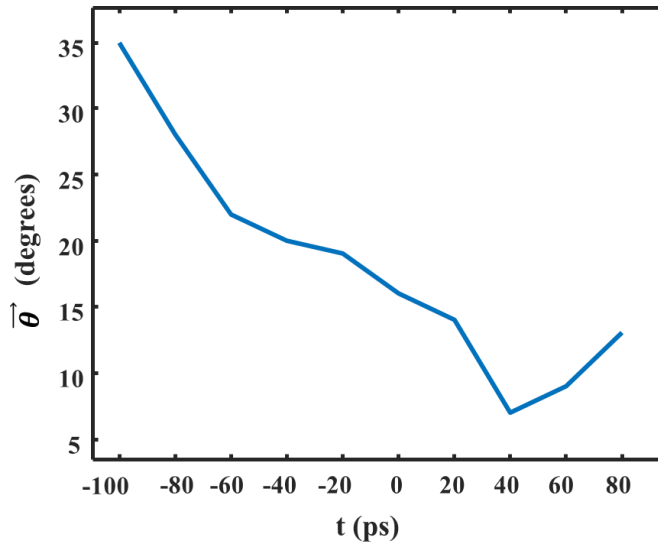
Fig. S3 Phase rotation angle variation curve of spatial vortex pulse.